

## Combined UV catalytic ozonation process on iron loaded peanut shell ash for the removal of methylene blue from aqueous solution

Amir Ikhlāq<sup>a,\*</sup>, Farhan Javed<sup>b,\*</sup>, Ayesha Niaz<sup>a</sup>, Hafiz Muhammad Shahzad Munir<sup>c</sup>, Fei Qi<sup>d</sup>

<sup>a</sup>Institute of Environmental Engineering and Research, University of Engineering and Technology, GT Road, 54890 Lahore, Pakistan, emails: aamirikhlaq@uet.edu.pk (A. Ikhlāq), ayeshaniiaz05@gmail.com (A. Niaz)

<sup>b</sup>Department of Chemical and Polymer Engineering, University of Engineering and Technology, Faisalabad Campus, 38000 Lahore, Pakistan, Tel. +92412433508; email: farhan.javed@uet.edu.pk (F. Javed)

<sup>c</sup>Department of Chemical Engineering, Khwaja Fareed University of Engineering and Information Technology (KFUEIT), Abu Dhabi Road, Rahim Yar Khan 64200, Pakistan, email: engrsm124@gmail.com (H.M.S. Munir)

<sup>d</sup>Beijing Forestry University, No. 35 Qinghua East Road, Haidian District, Beijing 100083, P.R. China, email: qifei\_hit@163.com (F. Qi)

Received 15 October 2019; Accepted 14 May 2020

### ABSTRACT

This study explores the effectiveness of peanut shell ash (PSA) as a catalyst for the removal of methylene blue (MB) using a synergistic photocatalytic process (UV/Fe-PSA/O<sub>3</sub>). The color and chemical oxygen demand (COD) removals were studied for ozonation and synergistic process, and the mechanism of the catalytic ozonation synergistic process was explained by studying the production of reactive oxygen species, such as hydroxyl radicals (HR), superoxide ion radicals (SOR), and hydrogen peroxide. The process comparison, scavenger effect, catalyst-dose effect, and pH effect were studied, and a mechanism was proposed. The synergistic process effectively performed 94% decolorization and 72.7% COD removal at pH 6 and 0.1 g Fe-PSA dose at room temperature. The pH studies showed effective performance of synergistic photocatalytic process at pH 4, 6, and 9, respectively, with the maximum efficiency at alkaline pH near the p*H*<sub>pzc</sub> of the catalyst. The process efficiency reduction by the addition of scavenger confirms that the UV-irradiated Fe-PSA based ozonation process follows a radical mechanism provoking the production of SORs and HRs. Therefore, it has been found that Fe-PSA/O<sub>3</sub> irradiated with UV radiation can act as a cheap alternative process for treating dye composed wastewater.

**Keywords:** Catalytic ozonation; Iron loaded peanut shell ash; Methylene blue; Reactive oxygen species; UV-irradiation

### 1. Introduction

The vast growth in industrialization is causing the release of non-biodegradable pollutants and toxic dyes which has become a major hazard to public and environmental health [1]. Water pollution control has become a major thrust area of scientific research and a rising awareness caused by emerging pollutants has been running globally. Therefore, the removal of these pollutants is a central step for wastewater treatment [2]. Different organic pollutants like dyes,

pharmaceuticals, and pesticides are difficult to treat due to their non-biodegradability [3–5]. Although different physical, biological, and chemical methods are available for the treatment of dyes however their specific nature towards specific pollutants varies [6,7].

Conventionally available methods are no longer effective for the treatment of biological resistant pollutants. Therefore, it is important to study novel methods available such as advanced oxidation processes (AOPs) which includes catalytic oxidation [8–10] Fenton process [11–13]

\* Corresponding authors.

and photocatalysis process [14], etc. AOPs have shown the efficient abatement of pollutants based on a radical mechanism [15]. AOPs combined with UV radiations have shown effective dye treatment in some studies [16]. Despite the increase in the use and research of advanced methods, there is a continuing need to develop novel economical catalysts and to investigate their mechanisms to imply them on a larger scale [17–19]. In the recent few years, to understand catalytic ozonation processes, studies were conducted to elucidate the generation of highly reactive oxygen species (ROS) in such processes [20,21]. It was found that the formation of various ROS like hydroxyl radicals (HRs) and superoxide ion radicals (SORs) plays an active role in the removal of various pollutants [21]. Studies indicate hydrogen peroxide may form in catalytic ozonation process that may have a negative influence on the removal of pollutants [22,23]. Therefore, catalytic processes that may help to decompose hydrogen peroxide causing the production of hydroxyl radicals may help to improve the overall effectiveness and economic benefits. In the current investigation UV-irradiated catalytic ozonation process using iron-loaded peanut shell ash (PSA) was tested as the catalyst. Hence because of UV-rays exposure and interactions with catalysts (iron on the catalyst) hydrogen peroxide decomposition may result. Recently, combine processes were used in catalytic oxidation processes to enhance the effectiveness of the process as compared to other methods (catalytic ozonation and ozonation alone) which when used alone, may not be highly effective in real conditions, due to inadequate oxidation capacity of ozone for some organic compounds [24,25]. Previous findings indicate that iron-loaded catalysts were found to be highly effective in catalytic ozonation system for the pollutant removal [26,27]. The surface hydroxyl groups on the iron platform may interact with aqueous ozone leading to the generation of hydroxyl radicals [26,27].

The iron-based catalysts are highly efficient for the wastewater treatment when applied in the catalytic ozonation process [28,29]. Iron-based heterogeneous catalysts effectively prolong the ozone residence time thereby increasing the ozone utilization and catalytic activity in catalytic ozonation processes [28]. Van et al. [29] reported reactive red 24 degradation by using iron slags heterogeneous catalytic ozonation and Fenton processes. Hundred percent mineralization was achieved in iron slags combined catalytic ozonation process at alkaline pH 11. Hien et al. [30] reported direct black 22 dye degradation by heterogeneous catalytic ozonation using metal slags such as Fe–S catalyst. The Fe–S combined ozonation achieved 90% decolorization and 70% chemical oxygen demand (COD) reduction [30]. Huang et al. [28] reported the effective mineralization of real pharmaceutical wastewater by employing iron foam combined catalytic ozonation. The COD and dissolved organic carbon removals of 70% and 54% were achieved respectively at pH 8.4, iron foam dosage 80 g/L, and 9 mg/L ozone concentration.

This study focusses on the removal of methylene blue by combined catalytic UV method using iron-loaded PSA as a catalyst. This is the continuation of the authors' previous study by utilizing PSA as a catalyst in AOPs. The previous study involves the application of Fe-PSA as a Fenton-like catalyst [31]. In the current investigation, Fe-PSA has been

selected for UV irradiated catalytic ozonation process. The sole purpose to select PSA as support was due to its unique nature since it contains a significant amount of silica and alumina [31]. That may give effective hydrophobic (silica) and hydrophilic (alumina) components in the process. Since previous findings suggested that catalytic ozonation processes may depend upon the adsorption of pollutants and the nature of adsorbent and adsorbate [32]. Moreover, PSA is an agricultural waste and is available in large quantities. This agriculture waste has been marked as potential adsorbent and can be used for the treatment of different pollutants [33–35]. PSA can be employed as a catalyst due to its high silica, alumina content and may bring economic and environmental benefits. To the best of author knowledge, Fe-coated PSA was not previously studied in the photocatalytic ozonation process. In catalytic ozonation processes, the nature of support (base material) PSA is important [36]. Since PSA has unique properties having silica and alumina contents that determine its hydrophobicity and hydrophilicity, respectively, which imparts an important role in the adsorption of pollutants of different types and surface reactions [36].

In this work, methylene blue (MB) was used as a targeted pollutant. MB is extensively used in industrial applications however, it gains attention due to its high toxicity and chronic effects. Efforts have been made to remove MB from the environment and to comply with international standards [37,38]. This research aims to elucidate the efficiency and effectiveness of the UV-irradiated catalytic ozonation process with iron-loaded PSA for the degradation of methylene blue and study the mechanism during the process. Additionally, the generation of ROS like HRs, SORs, and hydrogen peroxide was investigated to understand the mechanism of catalytic ozonation on Fe-PSA.

## 2. Methods

### 2.1. Materials and reagents

In the present research, the MB used was purchased from May and Baker, United Kingdom. A 30% hydrogen peroxide solution was procured from Merck, Germany. All reagents used were available at IEER lab UET Lahore. The pH of the solutions was set using 1 N NaOH and 1 N HCl.

### 2.2. Preparation of catalyst

Peanut shell, collected from a regional market in district Lahore, was washed with freshly prepared deionized water and then dried in a furnace at 660°C to convert it into ash. The unnecessary burned pieces were separated using a 45 µm sieve to get fine ash [39]. The PSA was prepared by following the method available in the literature [12,40]. The ash was immersed in a 0.1 N nitric acid solution for 24 h and then washed thoroughly with deionized water to remove impurities. The ash then dried overnight in an oven at 110°C. According to the method [41], 4.96 g of FeSO<sub>4</sub> was dissolved in 100 mL of deionized water to prepare a 0.176 M solution. Now by using impregnation method [42,43], 6.0 g of dried ash was taken, and 30 mL of prepared iron solution

was added. The solution was agitated at 100 rpm at 60°C until the water was evaporated with constant stirring for 6 h. The sample than dried overnight at 100°C for 6 h. The ash obtained was washed with deionized water and then dried overnight.

### 2.3. Catalyst characterization

The morphology and elemental properties both for PSA with and without iron were done using scanning electron microscopy (SEM) and energy dispersive X-ray spectroscopy (EDS) using JSM-6060A analyzer. The point of zero charge was evaluated using the mass transfer method [44]. The surface area was determined by the Brunauer–Emmett–Teller (BET) method using (Micro metrics USA, ASAP 2020).

### 2.4. Decolorization experiments

Experiments for dye removal were performed in a semi-batch reactor shown in Fig. 1. During the study, 400 mL of prepared solution of methylene blue (50 ppm for oxidation) was taken and the weighed amount of catalyst was poured in it. Ozone was fed in the reactor on a continuous rate for 15 min. The decolorization efficiencies of MB with and without the addition of hydroxyl radical scavenger (sodium bicarbonate, 100 ppm) were also investigated. The pH of the sample was adjusted using prepared solutions of 0.1 N NaOH and HCl. Samples were regularly taken after every minute, quenched with few drops of sodium carbonate to remove the un-reacted ozone. The solution is continuously stirred at 100 rpm using a magnetic stirrer at room temperature under UV irradiation. The samples were analyzed on double beam UV/Vis spectrophotometer Perkin-Elmer Lambda 35. Two traps of potassium iodide were also attached to find the concentration of gas. Finally, 10 mL of 1 N nitric acid was put in KI traps and titrated against 0.025 N sodium thiosulphate solution [45]. All experiments were carried out in a dark place and the reactor was also covered with light

resisting materials. The instruments were calibrated before analysis. Each experiment was performed thrice, and RSD was calculated and found to be less than 5%. All experiments were performed in the control environment.

The dye removal efficiency was determined by:

$$\text{Percentage Removal (\%)} = \frac{100 \times (C_0 - C_t)}{C_0} \quad (1)$$

where  $C_0$  is the zero-time absorbance,  $C_t$  is the  $t$  time absorbance.

### 2.5. Analytical procedures

#### 2.5.1. Analysis of methylene blue

The standard solution of 50 ppm concentration was prepared using a stock solution. The maximum absorbance was found by placing a small fraction of the prepared solution (50 ppm) in a silica cell. The calibration curve of the MB solution was obtained by making a standard solution from an already prepared stock solution of a suitable concentration range. The prepared standards were then analyzed on a UV-vis spectrophotometer at  $\lambda_{\text{max}}$  664 nm.

#### 2.5.2. COD estimation

COD of the real wastewater was done for 60 min for simple ozonation and catalytic ozonation. The standard method for COD estimation was followed. In order to avoid interferences, caused by catalytic ozonation, 4 mL of  $\text{MnO}_2$  were added during the process [45].

#### 2.5.3. Analysis of superoxide ion radical

The NBD-Cl product (formed by the NBD-Cl and superoxide ions reaction) was quantified in each sample by UV-vis spectroscopic method (Perkin-Elmer Lambda

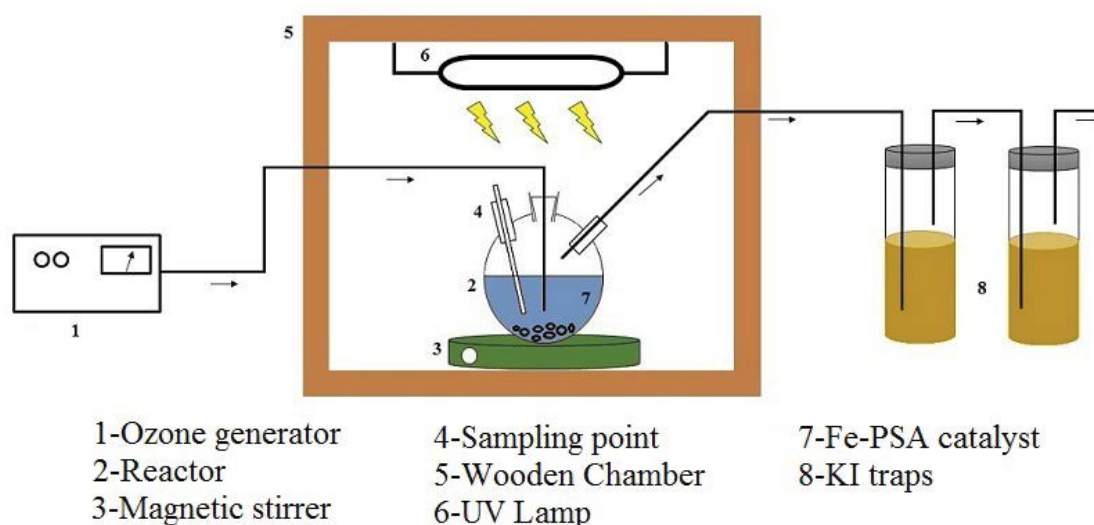


Fig. 1. Reactor setup. (1) Ozone generator, (2) reactor, (3) magnetic stirrer, (4) sampling point, (5) wooden chamber, (6) UV lamp, (7) Fe-PSA catalyst, and (8) KI traps.

35, UV/vis spectrophotometer) at 470 nm [46]. The samples were analyzed in a 1.0 cm cell. The NBD-Cl product formation was checked by calibrating samples  $\text{KO}_2$  (source of superoxide) and NBD-Cl. In order to quantify superoxide ion radical concentrations, NBD-Cl (20 ppm) was reacted (1:1 v/v) with solutions of different concentrations of superoxide ion (ranges from 0 to 7.2 ppm). The NBD-Cl product formed was analyzed by measuring absorbance at 470 nm, the calibration curve was prepared between absorbance (at 470 nm) against  $\cdot\text{O}_2^-$  concentration ( $\text{KO}_2$  concentrations were in 0–7.11 mg/L range) [46]. The concentrations of  $\cdot\text{O}_2^-$  radicals were quantified from the calibration curve.

#### 2.5.4. Analysis of resorufin/hydrogen peroxide

The  $\text{H}_2\text{O}_2$  concentration was evaluated by the resorufin fluorescence spectrum using a spectrometer (F-4500 Japan) with the slits set at 5 nm. Fluorescence was detected at 587 nm and calibration curves were drawn by reacting  $\text{H}_2\text{O}_2$  and amplex red reagent for 30 min as described elsewhere [46]. Based on previous findings [46] amplex red concentration 15 mg/L was taken. Since a significant amount of probe (amplex red) should always be present in the solution of such a system so that formed  $\text{H}_2\text{O}_2$  may promptly react with the probe.

### 3. Results and discussion

#### 3.1. Catalyst characterization

The point of zero charge of the catalyst is important in studies to understand the behavior of catalyst at various pH [47]. The point of zero charge of the catalyst used in this study was found to be  $9.1 \pm 0.4$ . Figs. 2a and b show the SEM images of PSA. SEM analysis of PSA shows that the surface morphology of the ash is unchanged even after the iron was incorporated on the ash [31]. The chemical composition of both PSA and Fe-PSA was studied using EDS, Fig. 3 confirms the presence of Fe on the catalyst. Additionally, Fig. 3 also shows the presence of other potential metals like aluminum (Al), zinc (Zn), and silicon (Si) that are important in this area of catalytic ozonation [48]. Furthermore, the surface area of the catalyst was  $18.13 \text{ m}^2/\text{g}$  with a pore size

having a diameter of 14.10 nm (Table 1). The PSA surface area was slightly decreased after iron coating due to the iron capping of pores [49] and also the pore diameter was increased.

#### 3.2. UV-irradiated catalytic ozonation using iron-loaded PSA

##### 3.2.1. Comparison between catalytic and non-catalytic process

It was observed that combining UV with the catalyst is more effective as compared to simple ozonation alone (Fig. 4). In the case of simple ozonation the maximum removal efficiency achieved after 3 min was 45%, whereas in the combined process, the removal was 60%. This may be due to the rise in the production of HRs due to molecular ozone interactions with the surface hydroxyl groups of iron-loaded PSA, which may cause the high decolorization efficiency of MB at studied pH as compared with single ozonation [20,21]. Moreover, the UV-irradiation further helps to decompose formed  $\text{H}_2\text{O}_2$  leading to the production of sufficient hydroxyl radicals [22,23,50]. Sumegová et al. [51] reported the oxidation of MB by comparing the ozonation with catalytic ozonation and showed that the efficiency and kinetics of ozonation are greatly accelerated due to catalyst. This study showed 71% MB decolorization efficiency by ozonation after 10 min and 78% in the presence of GAC catalytic ozonation. In the current study, after 10 min 75.6% MB decolorization was obtained in the ozonation process and 90.4% was achieved in the catalytic ozonation process while the cost of GAC is much higher as compared to PSA. Tichonovas et al. [52] reported MB degradation and showed that the photocatalytic ozonation process was the most efficient among photolysis, photocatalysis, photolytic ozonation, and catalytic ozonation.

##### 3.2.2. Hydroxyl radical scavenger effect

Hydroxyl radical scavengers were used in many findings to confirm the production of hydroxyl radicals in AOPs [53]. To elucidate the mechanism governing by the studied process ( $\text{O}_3/\text{UV}/\text{Fe-PSA}$ ), the decolorization efficiencies of MB with and without the addition of hydroxyl radical scavenger (sodium bicarbonate) were investigated [54]. The results clearly evidence that removal of MB was

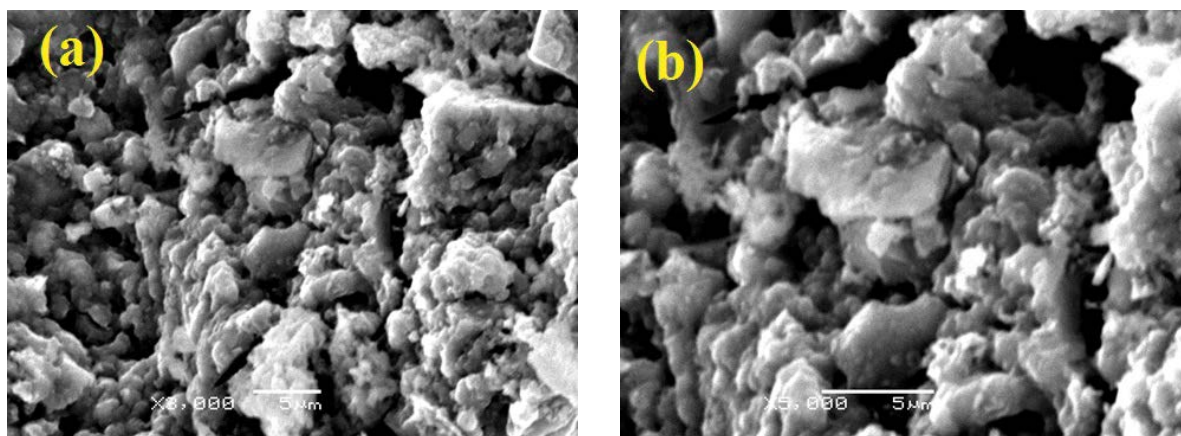


Fig. 2. SEM of (a) PSA and (b) Fe-PSA [24].

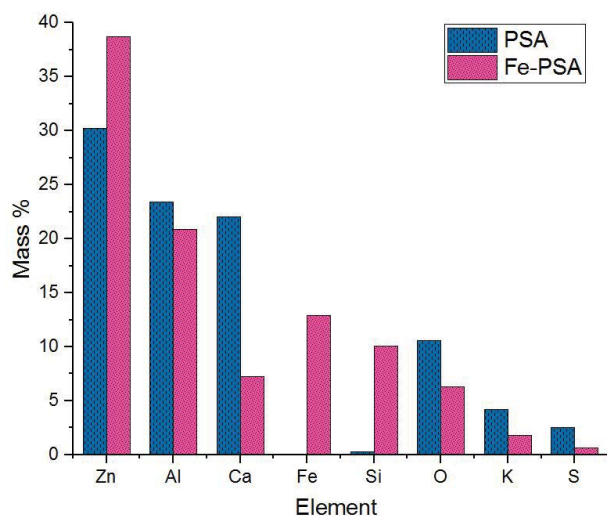
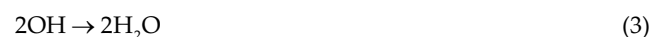


Fig. 3. EDS results of catalyst.

significantly by adding hydroxyl radical scavenger for the  $O_3$ /UV/Fe-PSA process as compared with single ozonation (Fig. 5). Therefore, the results show that by adding sodium bicarbonate the decolorization efficiency decreased, showing the prevalence of a radical mechanism in the case of  $O_3$ /UV/Fe-PSA process [46,54]. It may be hypothesized that hydroxyl radicals in the synergic process were produced not only by the interactions of ozone with catalyst surface OH groups, but also, ozone interactions with water molecules in solution with UV light may further results in the production of hydroxyl radicals [Eq. (2)]. Furthermore, the formed radicals in the synergic process may combine to produce hydrogen peroxide [Eq. (3)], which may dissociate into hydroxyl radicals again in the presence of UV rays [Eq. (4)].



$NaHCO_3$  is a radical scavenger and was implied previously in such studies. Fig. 5 shows that in the case of ozonation with the addition of the salt ( $NaHCO_3$ ), the decolorization efficiency was slightly increased as compared to that of ozonation without  $NaHCO_3$  addition. This may be because the dye decolorization is highly favored by the direct attack of ozone and the formation of hydroxyl radicals may be limited in  $NaHCO_3$  presence [55].

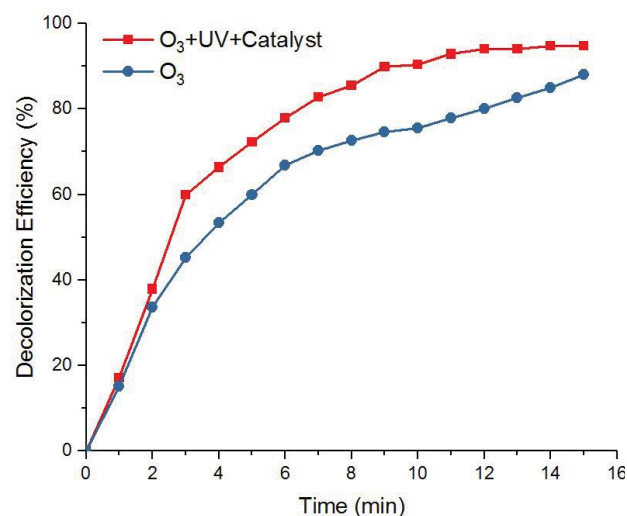


Fig. 4. Comparison between MB removal efficiencies of ozonation and combined UV catalytic ozonation ( $C_0$  (MB) = 50 mg/L, pH = 6, ozone supplied = 1 mg/min, volume = 400 mL, and catalyst dose = 0.1 g).

### 3.2.3. Removal of chemical oxygen demand

To confirm the degradation of MB during studied synergic process COD removal efficiencies were investigated (Fig. 6) [56,57]. Fig. 6 reveals that both simple and combined UV catalytic ozonation process remove COD effectively. However, COD removal was up to 72.7% in the case of the synergic process ( $O_3$ /UV/Fe-PSA) and only 50% in the case of simple ozonation. This shows that the degradation rate increased during the catalytic process as compared to ozonation alone, that may be due to the rise in the production of HRs in the synergic process as compared with single ozonation [46,54].

### 3.2.4. Effect of pH

The pH effect may play the main role in catalytic processes, since it may alter the mechanism of catalytic ozonation process, whether direct molecular ozone mechanism involves of radical based process. The surface charge of on a catalyst may be the function of pH of aqueous solution. Moreover, it determines whether the catalyst is protonated, deprotonated, or neutral in water [58]. In addition, the point of zero charge of adsorbent and charge on pollutant at particular pH may be significant for the adsorption of pollutant on the surface of the catalyst. Fig. 7 shows that the photocatalytic process was found to be highly efficient at all

Table 1  
PSA catalyst characteristics

Material	BET surface area ( $m^2/g$ )	Average pore diameter (nm)	Point of zero charge ( $pH_{pzc}$ )	Iron loading (weight %)
PSA	20.12	13.07	$8.3 \pm 0.4$	–
Fe-PSA	18.13	14.10	$9.1 \pm 0.4$	13.11

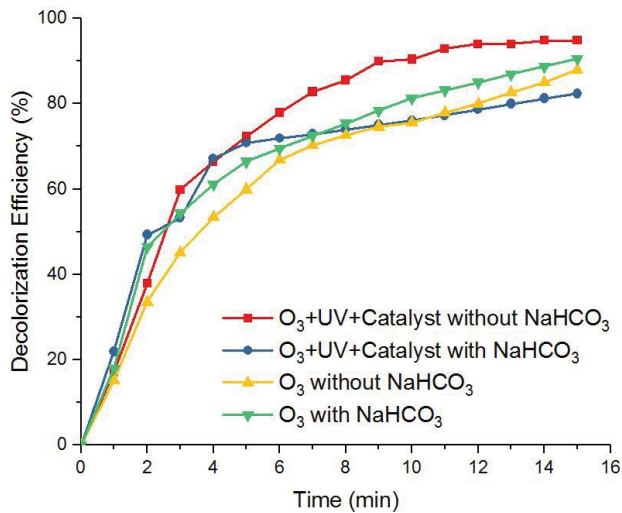


Fig. 5. Hydroxyl radical scavenger effect on removal of MB by adding sodium bicarbonate during simple ozonation and combine catalytic + UV process ( $C_0$  (MB) = 50 mg/L,  $C_{(\text{NaHCO}_3)}$  = 50 mg/L, pH = 6; catalyst dose = 0.1 g,  $O_3$  = 1 mg/min, and  $V$  = 400 mL).

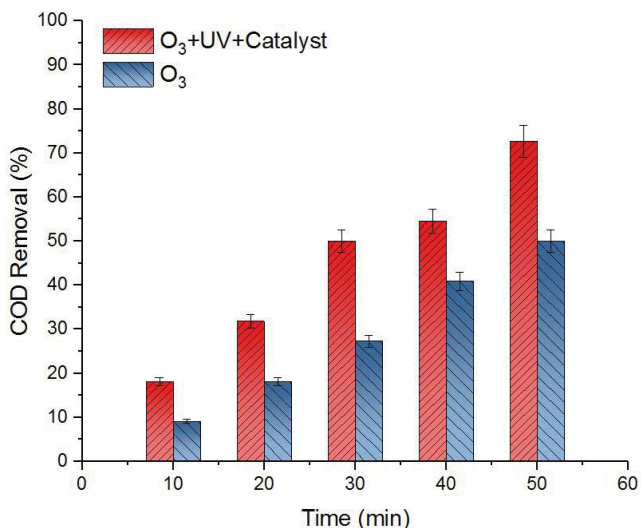


Fig. 6. Percentage removal of COD during simple ozonation and combine catalytic UV ozonation ( $O_3$  = 1 mg/min,  $C_0$  (MB) = 50 mg/L, pH = 6, catalyst dose = 0.1 g, and  $V$  = 400 mL).

operating pH. At acidic pH (pH = 4), although adsorption of MB was negligible (similar charge on adsorbate and adsorbent) however the removal efficiency was much higher in the photocatalytic process since at this pH more molecular ozone is available for UV-irradiation leading to the production of ROS [46]. While with the rise in pH the catalytic ozonation process dominates and at pH near the point of zero charge of catalyst, adsorption was significantly higher as compared to other pH values (Fig. 8), this may be due to lack of repulsive forces of similar charges (positive charge) near the point of zero charge [26]. Moreover, the catalytic activity may be better near the point of zero charge [46]. Therefore, the removal efficiency was found to be better at

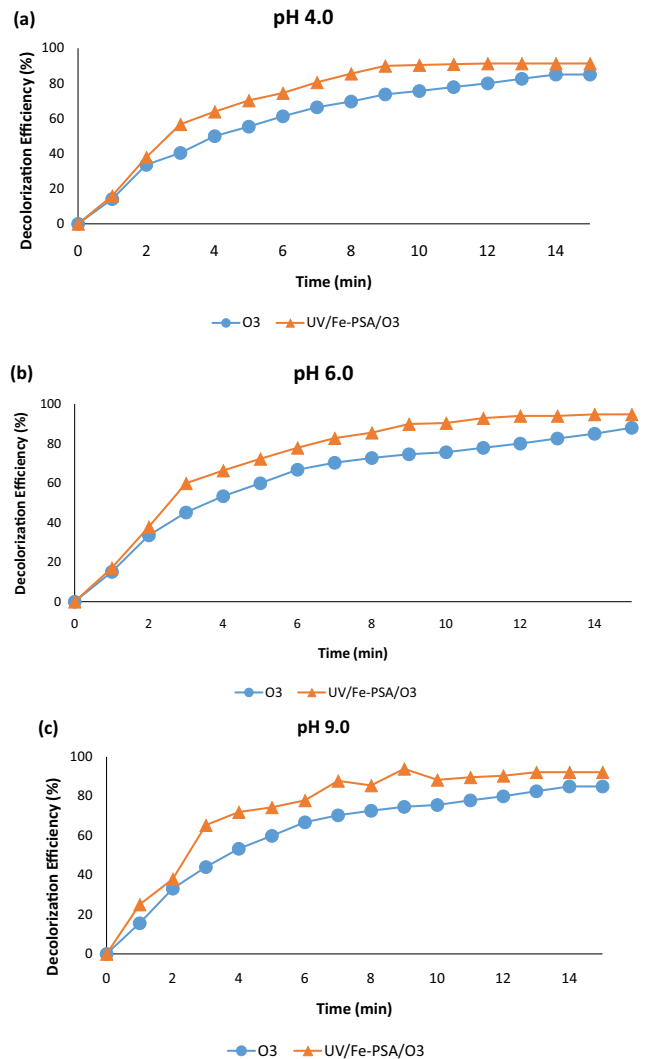


Fig. 7. Effect of studied pH on processes (a) pH 4, (b) pH 6, and (c) pH 9 ( $C_0$  (MB) = 50 mg/L, catalyst dose = 0.1 g,  $O_3$  = 1 mg/min,  $V$  = 400 mL, and  $T$  = 15 min).

pH near the point of zero charge as compared to other pH values.

Jaramillo-Sierra et al. [59] reported similar results. The study showed MB degradation in UV assisted ozonation was greatly affected by the pH and the highest degradation was achieved at pH 9 due to activated breakdown of  $O_3$  to OH radicals.

### 3.2.5. Catalytic dose effect

To analyze the effect of the added amount of catalyst during combine catalytic and UV ozonation, the number of experiments carried out using catalyst dose of 0.03, 0.1, and 1 g in a semi-batch reactor near wastewater pH (pH = 6–9). Fig. 9 indicates that the removal of methylene blue enhances with the rise in catalyst dose. For example, the decolorization of MB was found to be 94%, 64%, and 53% for 1, 0.1, and 0.03 g, respectively (in the first 5 min of ozonation). This may be because of the increase in catalyst dose that

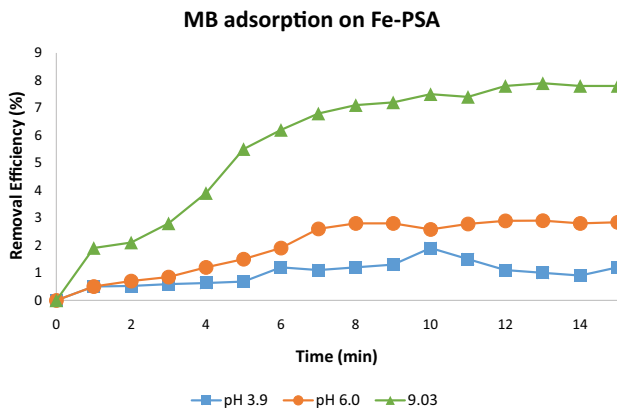


Fig. 8. MB adsorption on Fe-PSA at studied pH ( $C_0$  (MB) = 50 mg/L, pH = 3.9, 6.0, 9.03, Fe-PSA dose = 0.1 g, and  $V = 400$  mL).

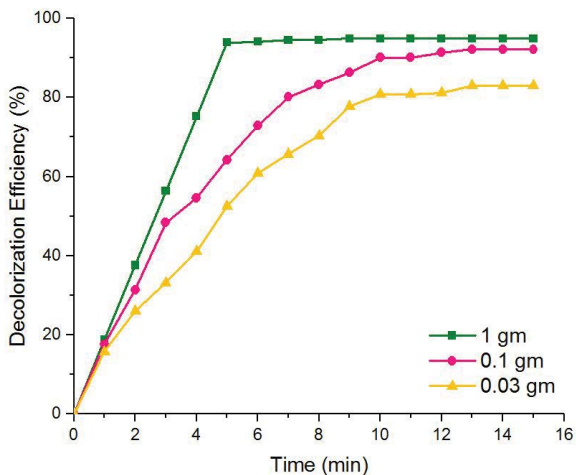


Fig. 9. Comparison between decolorization efficiencies of MB in combined UV catalytic ozonation process at various catalyst doses ( $C_0$  (MB) = 50 mg/L,  $O_3 = 1$  mg/min, pH = 6, volume = 400 mL, catalyst dose = 0.03, 0.1, and 1 g).

may raise number of active sites which leads to the increase in ozone decomposition accelerating the production of HRs [58,60]. Therefore, the results further confirm the significant catalytic activity of Fe-PSA for the decolorization of dyes. Liu et al. [61] reported similar results on catalytic ozone decomposition of MB. The study showed MB removal after 10 min were 70% at 0.3 g catalyst dose and enhanced to more than 85% at 0.7 g catalyst dose. The present study showed that after 10 min the MB removal was increased from 80.8% at 0.03 g dose to 94.9% at 1 g dose.

### 3.2.6. Catalyst reusability

The Fe-PSA catalytic reuse performance was studied in the synergic (UV/Fe-PSA/ $O_3$ ) process for three successive cyclic runs. Fig. 10 represents the obtained results showing that there was a slight reduction in the catalytic performance of Fe-PSA after reuse, and removal efficiency of 86.5% was

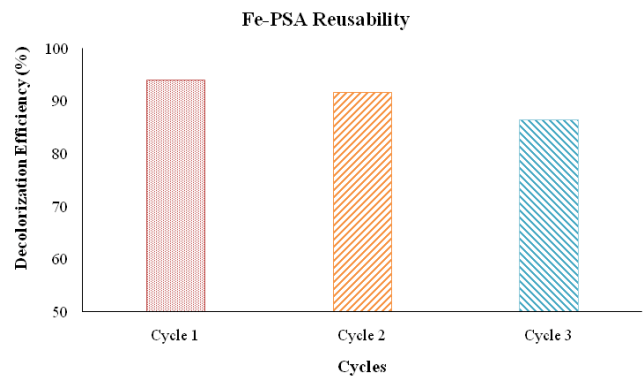


Fig. 10. Fe-PSA reusability process ( $C_0$  (MB) = 50 mg/L, pH = 9, catalyst dose = 0.1 g,  $O_3 = 1$  mg/min,  $V = 400$  mL, and  $T = 15$  min).

achieved after cycle 3. The slight decrease in the Fe-PSA catalytic performance may be attributed to the iron leach out effect [62].

### 3.2.7. Production of superoxide ion radicals and hydrogen peroxide

Fig. 11a shows the production of SOR in studied processes, it clearly shows that a significant quantity of  $\cdot O_2^-$  radical ions was formed in the synergic process (UV/ $O_3$ /Fe-PSA) as compared with single ozonation which may be due to the interactions of hydroxyl ions on the catalyst surface, with molecular ozone that may result in the production of significantly higher  $\cdot O_2^-$  radical ions at studied pH (pH = 6) [13,32]. The decrease in  $\cdot O_2^-$  radical ions after 10 min of ozonation (Fig. 11a) may be due to the interactions between the probe (NBD-Cl) with ozone and hydroxyl radicals [20].

To further confirm the effectiveness of the studied synergic process, the formation of hydrogen peroxide was investigated during the various processes. The results presented in Fig. 11b suggest that in all processes that are single ozonation, catalytic ozonation and UV-irradiated catalytic ozonation significant amount of hydrogen peroxide may be produced. This may be because formed hydroxyl radicals may combine to produce  $H_2O_2$ , which may negatively affect the processes efficiency since  $H_2O_2$  has less rate of reaction as compared with hydroxyl radicals [22,23]. Interestingly, Fig. 11b reveals that the production of  $H_2O_2$  significantly decreased after 30 min in the synergic process as compared with single processes. This may be due to  $H_2O_2$  decomposition in the presence of UV-rays [Eq. (4)] leading to the generation of HRs, this further supports our hypothesis that high effectiveness of synergic process may be due to the production of  $H_2O_2$  in low quantity and its decomposition causing the formation of hydroxyl radicals.

### 3.3. Proposed mechanism

Fig. 12 shows the mechanism involved in the synergic process. It has been proposed that ozone may engage with the surface hydroxyl groups on iron leading to the production of superoxide ion radical. Interestingly, the increase in the generation of superoxide ion in catalytic ozonation and

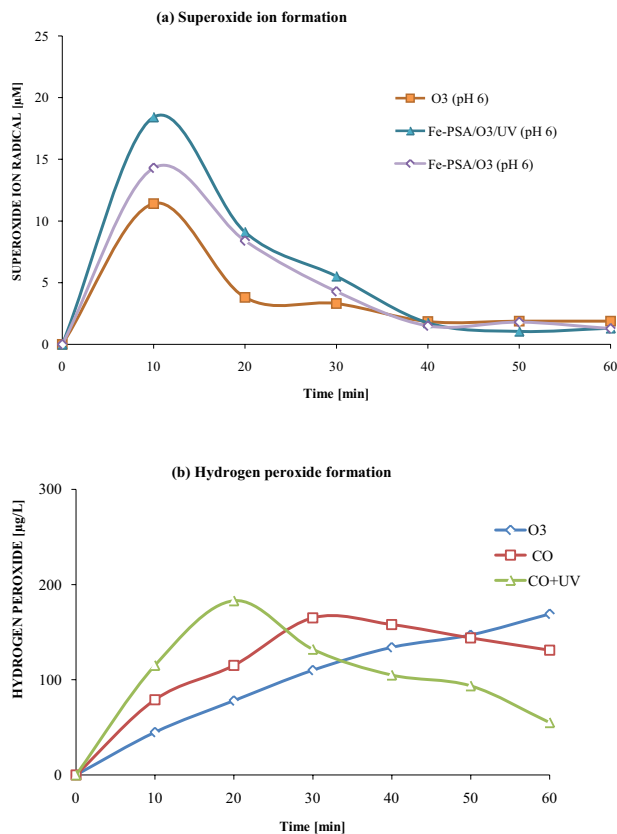


Fig. 11. Formation of (a) superoxide ion radicals and (b) hydrogen peroxide in single ozonation, catalytic ozonation, and UV assisted catalytic ozonation processes ( $C_{0\text{Amplex red}} = 15 \text{ mg/L}$ , pH = 6, ozone supplied = 1 mg/min, volume = 400 mL, catalyst dose = 0.1 g, and  $T = 20^\circ\text{C}$ ).

synergic process in comparison to single ozonation clearly support our hypothesis (Fig. 11a). The formed SOR further interact with molecular ozone leading to the generation of HRs [46,53]. The study of the hydroxyl radical scavenger effect clearly supports the findings that indicate the radical scavenger effect was the highest in the case of the synergic process (Fig. 5). Fig. 11 further reflects that the produced hydroxyl radicals may combine leading to the formation of hydrogen peroxide [22,23], which than dissociate into radicals in the presence of UV-rays as well as due to Fenton-like interactions with the active sites on Fe-PSA. This made the synergic process highly efficient as compared with catalytic ozonation and single ozonation.

#### 4. Conclusions

Main conclusions are drawn from the above research:

- Synergic process (UV/O<sub>3</sub>/Fe-PSA) showed effective results for the methylene blue removal with up to 94% decolorization and 72.7% COD removal at pH 6 and 0.1 g Fe-PSA dose.
- The addition of 50 mg/L of NaHCO<sub>3</sub> radical scavenger significantly reduced the decolorization efficiency which confirms that the UV-irradiated Fe-PSA based ozonation

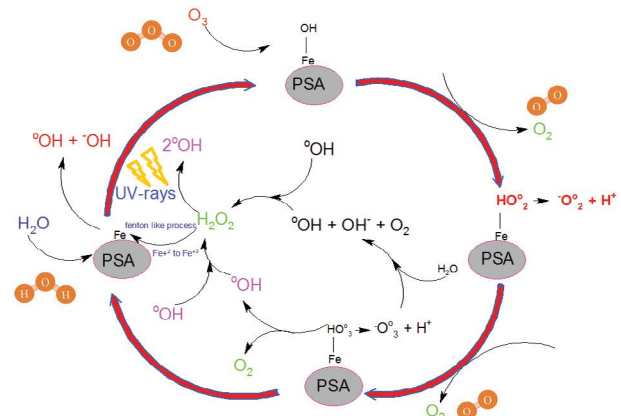


Fig. 12. Proposed mechanism of UV-irradiated catalytic ozonation with iron-loaded peanut shell ash.

process follows a radical mechanism provoking the production of SORs and HRs.

- The pH effect studies showed that the synergic process (UV/O<sub>3</sub>/Fe-PSA) is pH dependent. At pH = 9, which is near  $\text{pH}_{\text{PZC}}$  of catalyst, the catalytic ozonation process dominates and adsorption is also significant due to the lack of molecular repulsion.
- The decomposition of hydrogen peroxide in the synergic process increases the effectiveness of the synergic process.

#### Acknowledgment

The contribution of the staff and management of the University of Engineering and Technology, Lahore (Pakistan) is greatly acknowledged.

#### References

- [1] M. Grassi, G. Kaykioglu, V. Belgiorno, G. Lofrano, Removal of Emerging Contaminants from Water and Wastewater by Adsorption Process, G. Lofrano, Ed., Emerging Compounds Removal from Wastewater, Springer, Dordrecht, 2012, pp. 15–37.
- [2] K. Kümmerer, The presence of pharmaceuticals in the environment due to human use – present knowledge and future challenges, J. Environ. Manage., 90 (2009) 2354–2366.
- [3] K.E. Murray, S.M. Thomas, A.A. Bodour, Prioritizing research for trace pollutants and emerging contaminants in the freshwater environment, Environ. Pollut., 158 (2010) 3462–3471.
- [4] D. Kanakaraju, B.D. Glass, M. Oelgemöller, Advanced oxidation process-mediated removal of pharmaceuticals from water: a review, J. Environ. Manage., 219 (2018) 189–207.
- [5] Y. Anjaneyulu, N.S. Chary, D.S.S. Raj, Decolourization of industrial effluents – available methods and emerging technologies – a review, Rev. Environ. Sci. Biotechnol., 4 (2005) 245–273.
- [6] K. Ikehata, M.G. El-Din, S.A. Snyder, Ozonation and advanced oxidation treatment of emerging organic pollutants in water and wastewater, Ozone Sci. Eng., 30 (2008) 21–26.
- [7] N.K. Daud, B.H. Hameed, Decolorization of acid red 1 by Fenton-like process using rice husk ash-based catalyst, J. Hazard. Mater., 176 (2010) 938–944.
- [8] S. Yang, H. He, D. Wu, D. Chen, X. Liang, Z. Qin, M. Fan, J. Zhu, P. Yuan, Decolorization of methylene blue by heterogeneous Fenton reaction using  $\text{Fe}_{3-x}\text{Ti}_x\text{O}_4$  ( $0 \leq x \leq 0.78$ ) at neutral pH values, Appl. Catal., B, 89 (2009) 527–535.



- [9] P.V. Nidheesh, R. Gandhimathi, S.T. Ramesh, Degradation of dyes from aqueous solution by Fenton processes: a review, *Environ. Sci. Pollut. Res.*, 20 (2013) 2099–2132.
- [10] F. Çiçek, D. Özer, A. Özer, A. Özer, Low cost removal of reactive dyes using wheat bran, *J. Hazard. Mater.*, 146 (2007) 408–416.
- [11] R. Gonzalez-Olmos, M.J. Martin, A. Georgi, F.-D. Kopinke, I. Oller, S. Malato, Fe-zeolites as heterogeneous catalysts in solar Fenton-like reactions at neutral pH, *Appl. Catal., B*, 125 (2012) 51–58.
- [12] E.G. Garrido-Ramírez, B.K.G. Theng, M.L. Mora, Clays and oxide minerals as catalysts and nanocatalysts in Fenton-like reactions – a review, *Appl. Clay Sci.*, 47 (2010) 182–192.
- [13] A. Ikhlāq, H.M.S. Munir, A. Khan, F. Javed, K.S. Joya, Comparative study of catalytic ozonation and Fenton-like processes using iron-loaded rice husk ash as catalyst for the removal of methylene blue in wastewater, *Ozone Sci. Eng.*, 41 (2019) 250–260.
- [14] J. Hong, C. Sun, S.-G. Yang, Y.-Z. Liu, Photocatalytic degradation of methylene blue in TiO<sub>2</sub> aqueous suspensions using microwave powered electrodeless discharge lamps, *J. Hazard. Mater.*, 133 (2006) 162–166.
- [15] E. Basturk, M. Karatas, Advanced oxidation of Reactive Blue 181 solution: a comparison between Fenton and Sono-Fenton Process, *Ultrason. Sonochem.*, 21 (2014) 1881–1885.
- [16] E. Basturk, M. Karatas, Decolorization of anthraquinone dye reactive blue 181 solution by UV/H<sub>2</sub>O<sub>2</sub> process, *J. Photochem. Photobiol., A*, 299 (2015) 67–72.
- [17] J. Nawrocki, B. Kasprzyk-Hordern, The efficiency and mechanisms of catalytic ozonation, *Appl. Catal., B*, 99 (2010) 27–42.
- [18] S.M.H. Asl, A. Ghadi, M.S. Baei, H. Javadian, M. Maghsudi, H. Kazemian, Porous catalysts fabricated from coal fly ash as cost-effective alternatives for industrial applications: a review, *Fuel*, 217 (2018) 320–342.
- [19] P.V. Nidheesh, Graphene-based materials supported advanced oxidation processes for water and wastewater treatment: a review, *Environ. Sci. Pollut. Res.*, 24 (2017) 27047–27069.
- [20] A. Ikhlāq, S. Waheed, K.S. Joya, M. Kazmi, Catalytic ozonation of paracetamol on zeolite A: non-radical mechanism, *Catal. Commun.*, 112 (2018) 15–20.
- [21] Y. Deng, R. Zhao, Advanced oxidation processes (AOPs) in wastewater treatment, *Curr. Pollut. Rep.*, 1 (2015) 167–176.
- [22] T.-M. Hwang, B.S. Oh, Y. Yoon, M. Kwon, J. Kang, Continuous determination of hydrogen peroxide formed in advanced oxidation and electrochemical processes, *Desal. Water Treat.*, 43 (2012) 267–273.
- [23] H. Zhao, G. Zhang, Q. Zhang, MnO<sub>2</sub>/CeO<sub>2</sub> for catalytic ultrasonic degradation of methyl orange, *Ultrason. Sonochem.*, 21 (2014) 991–996.
- [24] C. Wei, F. Zhang, Y. Hu, C. Feng, H. Wu, Ozonation in water treatment: the generation, basic properties of ozone and its practical application, *Rev. Chem. Eng.*, 33 (2017) 49–89.
- [25] R.R. Solís, F.J. Rivas, A. Martínez-Piernas, A. Agüera, Ozonation, photocatalysis and photocatalytic ozonation of diuron. Intermediates identification, *Chem. Eng. J.*, 292 (2016) 72–81.
- [26] A. Alver, A. Kilic, Catalytic ozonation by iron coated pumice for the degradation of natural organic matters, *Catalysts*, 8 (2018) 219.
- [27] J. Wang, Z. Bai, Fe-based catalysts for heterogeneous catalytic ozonation of emerging contaminants in water and wastewater, *Chem. Eng. J.*, 312 (2017) 79–98.
- [28] Y. Huang, J. Jiang, L. Ma, Y. Wang, M. Liang, Z. Zhang, L. Li, Iron foam combined ozonation for enhanced treatment of pharmaceutical wastewater, *Environ. Res.*, 183 (2020) 109205.
- [29] H.T. Van, L.H. Nguyen, T.K. Hoang, T.P. Tran, A.T. Vo, T.T. Pham, X.C. Nguyen, Using FeO-constituted iron slag wastes as heterogeneous catalyst for Fenton and ozonation processes to degrade reactive red 24 from aqueous solution, *Sep. Purif. Technol.*, 224 (2019) 431–442.
- [30] N.T. Hien, L.H. Nguyen, H.T. Van, T.D. Nguyend, T.H.V. Nguyend, T.H.H. Chud, T.V. Nguyen, V.T. Trinh, X.H. Vu, K.H.H. Aziz, Heterogeneous catalyst ozonation of direct black 22 from aqueous solution in the presence of metal slags originating from industrial solid wastes, *Sep. Purif. Technol.*, 233 (2020) 115961.
- [31] A. Ikhlāq, H.Z. Anwar, F. Javed, S. Gull, Degradation of safranin by heterogeneous Fenton processes using peanut shell ash based catalyst, *Water Sci. Technol.*, 79 (2019) 1367–1375.
- [32] A. Ikhlāq, D.R. Brown, B. Kasprzyk-Hordern, Catalytic ozonation for the removal of organic contaminants in water on alumina, *Appl. Catal., B*, 165 (2015) 408–418.
- [33] L.G. Devi, S.G. Kumar, K.M. Reddy, C. Munikrishnappa, Photo degradation of methyl orange an azo dye by advanced Fenton process using zero valent metallic iron: influence of various reaction parameters and its degradation mechanism, *J. Hazard. Mater.*, 164 (2009) 459–467.
- [34] L.G. Devi, K.S.A. Raju, S.G. Kumar, K.E. Rajashekhar, Photo-degradation of di azo dye Bismarck brown by advanced photo-Fenton process: influence of inorganic anions and evaluation of recycling efficiency of iron powder, *J. Taiwan Inst. Chem. Eng.*, 42 (2011) 341–349.
- [35] Y. Yao, L.W.L. Sun, S. Zhu, Z. Huang, Y. Mao, W. Lu, W. Chen, Efficient removal of dyes using heterogeneous Fenton catalysts based on activated carbon fibers with enhanced activity, *Chem. Eng. Sci.*, 101 (2013) 424–431.
- [36] A. Ikhlāq, B. Kasprzyk-Hordern, Catalytic ozonation of chlorinated VOCs on ZSM-5 zeolites and alumina: formation of chlorides, *Appl. Catal., B*, 200 (2017) 274–282.
- [37] T.M. Albayati, A.A. Sabri, R.A. Alazawi, Separation of methylene blue as pollutant of water by SBA-15 in a fixed-bed column, *Arabian J. Sci. Eng.*, 41 (2016) 2409–2415.
- [38] S. Tian, J. Zhang, J. Chen, L. Kong, F. Ding, Y. Xiong, Fe<sub>2</sub>(MoO<sub>4</sub>)<sub>3</sub> as an effective photo-Fenton-like catalyst for the degradation of anionic and cationic dyes in a wide pH range, *Ind. Eng. Chem. Res.*, 52 (2013) 13333–13341.
- [39] G. Ersöz, Fenton-like oxidation of reactive black 5 using rice husk ash based catalyst, *Appl. Catal., B*, 147 (2014) 353–358.
- [40] D. Özer, G. Dursun, A. Özer, Methylene blue adsorption from aqueous solution by dehydrated peanut hull, *J. Hazard. Mater.*, 144 (2007) 171–179.
- [41] A. Ikhlāq, M. Anis, F. Javed, H. Ghani, H.M.S. Munir, K. Ijaz, Catalytic ozonation for the treatment of municipal wastewater by iron loaded zeolite A, *Desal. Water Treat.*, 152 (2019) 108–115.
- [42] A. Ikhlāq, M. Kazmi, A. Tufail, H. Fatima, K.S. Joya, Application of peanut shell ash as a low-cost support for fenton-like catalytic removal of methylene blue in wastewater, *Desal. Water Treat.*, 111 (2018) 338–334.
- [43] M. Rafatullah, O. Sulaiman, R. Hashim, A. Ahmad, Adsorption of methylene blue on low-cost adsorbents: a review, *J. Hazard. Mater.*, 177 (2010) 70–80.
- [44] K. Periasamy, C. Namasivayam, Removal of copper(II) by adsorption onto peanut hull carbon from water and copper plating industry wastewater, *Chemosphere*, 32 (1996) 769–789.
- [45] A.D. Eaton, Standard Methods for the Examination of Water and Wastewater, American Public Health Association, Water Environment Federation, USA, 1915.
- [46] A. Ikhlāq, D.R. Brown, B. Kasprzyk-Hordern, Mechanisms of catalytic ozonation: an investigation into superoxide ion radical and hydrogen peroxide formation during catalytic ozonation on alumina and zeolites in water, *Appl. Catal., B*, 129 (2013) 437–449.
- [47] F.Z. Yehia, G. Eshaq, A.M. Rabie, A.H. Mady, A.E. El-Metwally, Phenol degradation by advanced Fenton process in combination with ultrasonic irradiation, *Egypt. J. Pet.*, 24 (2015) 13–18.
- [48] M. Hermanek, R. Zboril, I. Medrik, J. Pechousek, C. Gregor, Catalytic efficiency of iron(III) oxides in decomposition of hydrogen peroxide: competition between the surface area and crystallinity of nanoparticles, *J. Am. Chem. Soc.*, 129 (2007) 10929–10936.
- [49] F. Adam, J. Andas, I.A. Rahman, A study on the oxidation of phenol by heterogeneous iron silica catalyst, *Chem. Eng. J.*, 165 (2010) 658–667.
- [50] R. Andreozzi, V. Caprio, R. Marotta, D. Vogna, Paracetamol oxidation from aqueous solutions by means of ozonation and H<sub>2</sub>O<sub>2</sub>/UV system, *Water Res.*, 37 (2003) 993–1004.

- [51] L. Sumegová, J. Derco, M. Melicher, Influence of reaction conditions on the ozonation process, *Acta Chim. Slov.*, 6 (2013) 168–172.
- [52] M. Tichonovas, E. Krugly, D. Jankunaite, V. Racys, D. Martuzevicius, Ozone-UV-catalysis based advanced oxidation process for wastewater treatment, *Environ. Sci. Pollut. Res.*, 24 (2017) 17584–17597.
- [53] A. Alver, E. Basturk, Removal of aspartame by catalytic ozonation with nano-TiO<sub>2</sub> coated pumice, *Desal. Water Treat.*, 152 (2019) 268–275.
- [54] C. Chen, X. Yan, B.A. Yoza, T. Zhou, Y. Li, Y. Zhan, Q. Wang, Q.X. Li, Efficiencies and mechanisms of ZSM5 zeolites loaded with cerium, iron, or manganese oxides for catalytic ozonation of nitrobenzene in water, *Sci. Total Environ.*, 612 (2018) 1424–1432.
- [55] J.B. Parsa, S.H. Negahdar, Treatment of wastewater containing acid blue 92 dye by advanced ozone-based oxidation methods, *Sep. Purif. Technol.*, 98 (2012) 315–320.
- [56] N.A.S. Amin, J. Akhtar, H.K. Rai, Screening of combined zeolite-ozone system for phenol and COD removal, *Chem. Eng. J.*, 158 (2010) 520–527.
- [57] M. Lim, Y. Son, J. Khim, Frequency effects on the sonochemical degradation of chlorinated compounds, *Ultrason. Sonochem.*, 18 (2011) 460–465.
- [58] E. Basturk, M. Işık, M. Karatas, Removal of aniline (methylene blue) and azo (reactive red 198) dyes by photocatalysis via nano TiO<sub>2</sub>, *Desal. Water Treat.*, 143 (2019) 306–313.
- [59] B. Jaramillo-Sierra, A. Mercado-Cabrera, A.N. Hernández-Arias, R. Peña-Eguiluz, R. López-Callejas, B.G. Rodríguez-Méndez, R. Valencia-Alvarado, Methylene blue degradation assessment by advanced oxidation methods, *J. Appl. Res. Technol.*, 17 (2019) 172–179.
- [60] G. Asgari, A. Rahmani, F.B. Askari, K. Godini, Catalytic ozonation of phenol using copper coated pumice and zeolite as catalysts, *J. Res. Health Sci.*, 12 (2012) 93–97.
- [61] X. Liu, Y. Hou, J. Guo, Y. Wang, Q. Zuo, C. Wang, Catalytic ozone aqueous decomposition of methylene blue using composite metal oxides, *IOP Conf. Ser.: Mater. Sci. Eng.*, 87 (2015) 012031.
- [62] K. Kruanak, C. Jarusutthirak, Degradation of 2,4,6-trichlorophenol in synthetic wastewater by catalytic ozonation using alumina supported nickel oxides, *J. Environ. Chem. Eng.*, 7 (2019) 102825.